Journal of Constructional Steel Research 101 (2014) 304–313

Contents lists available at ScienceDirect

Journal of Constructional Steel Research

Seismic retrofit design method for RC buildings using buckling-restrained braces and steel frames

Fatih Sutcu [a,*], Toru Takeuchi [b], Ryota Matsui [b]

[a] Department of Architecture, Istanbul Technical University, Turkey
[b] Graduate School of Engineering, Tokyo Institute of Technology, Japan

ARTICLE INFO

Article history:
Received 17 January 2014
Accepted 31 May 2014
Available online xxxx

Keywords:
Buckling-restrained braces
Retrofitting RC buildings
Residual displacement
Equivalent linearization
Nonlinear time history analysis
Elastically designed steel frames

ABSTRACT

Existing RC buildings conforming to relatively older regulations and codes may lack in seismic resistance. This is especially true for public buildings such as schools or hospitals, which demand efficient retrofitting to ensure safety during and after a seismic event. Although retrofit design with conventional braces (CB) has been practiced for decades, the unbalanced hysteresis behavior of CBs tends to result in damage concentrated in specific stories. Buckling-restrained braces (BRBs), a new generation of bracing system, may increase structural integrity and at the same time reduce seismic response in a building via energy absorption. However, when the maximum story drift exceeds the yield point of RC frame, all structural elements including BRBs lose horizontal stiffness, which may result in both damage at a specific story and residual deformation effects occurring after an earthquake. Therefore, BRBs may be applied to such buildings using elastically designed steel frames (SF).This paper discusses the evaluation of damage distribution and self-centering functions of the elastic steel frames that connect BRBs to RC frames. In addition, we propose a simplified method based on equivalent linearization to design the required amount of BRB and elastic SF capacity for retrofitting existing RC buildings. The results were confirmed by nonlinear time-history analysis using high-intensity seismic waves. The results show that RC buildings retrofit with BRBs respond as predicted by the proposed method and target story drift is obtained. The story drifts of the BRB retrofit model is significantly reduced relative to both the original building and the building retrofit with CBs. In addition, because BRBs are attached to an existing building by elastically designed steel frames, the significant effect of SF on the reduction of residual displacements was also shown and discussed.

1. Introduction

Catastrophic earthquakes in the past two decades have resulted in life and economic losses worldwide, which has led to evermore comprehensive seismic building codes and regulations being introduced in nearly every region. However, existing buildings that are not constructed according to these codes lack in seismic resistance, as observed during surveys performed after recent earthquakes. Therefore, it is important to retrofit buildings and enhance their seismic performance. Existing framed structures may be suitably retrofit using diagonal braces. However, owing to buckling of the brace compression members and material softening, the hysteretic behavior of conventional steel braces is unreliable. Alternatively, buckling-restrained braces (BRBs) being elasto-plastic dampers may be employed as diagonal braces in the seismic retrofitting of steel and RC frames designed for gravity loads only.

Previous researchers have proposed simplified theories to predict the seismic performance of passive response control systems. For such purposes, the equivalent damping and period of these systems are idealized as single-degree-of-freedom (SDOF) systems or other equivalent linearization methods [1–4]. In a study presented by Choi and Kim [5], an energy-based seismic design procedure for framed structures with BRBs is proposed using hysteretic energy spectra and accumulated ductility spectra. The proposed method assumes that beams and columns are designed to remain elastic during an earthquake and that all seismic input energy is dissipated by the BRBs. In another study, Sahoo and Chao [6] presented a performance-based plastic design methodology for the design of buckling-restrained braced frames, where design-based shear is obtained via an energy–work balance using preselected target drift and yield mechanisms. However, these studies are based on an elastic building model, such as steel buildings. Pu and Kasai [7] proposed a passive control design method for seismic response evaluation and the preliminary design of RC buildings with elasto-plastic dampers, in which seven- and seventeen-story RC building models were used. Pu and Kasai present a method to convert an idealized SDOF design into a multi-story design by considering the distribution of damper stiffness over the building height. Others have modeled the effects of BRBs and CBs on structural performance and compared the results. Prinz and

* Corresponding author at: Structural and Earthquake Engineering Working Group, Department of Architecture 103, Istanbul Technical University, 34437, Turkey. Tel.: +90 212 2931300x2281; fax: +90 212 2514895.
E-mail addresses: fatih.sutcu@itu.edu.tr (F. Sutcu), ttoru@arch.titech.ac.jp (T. Takeuchi), matsui.r.aa@m.titech.ac.jp (R. Matsui).

http://dx.doi.org/10.1016/j.jcsr.2014.05.023
0143-974X/

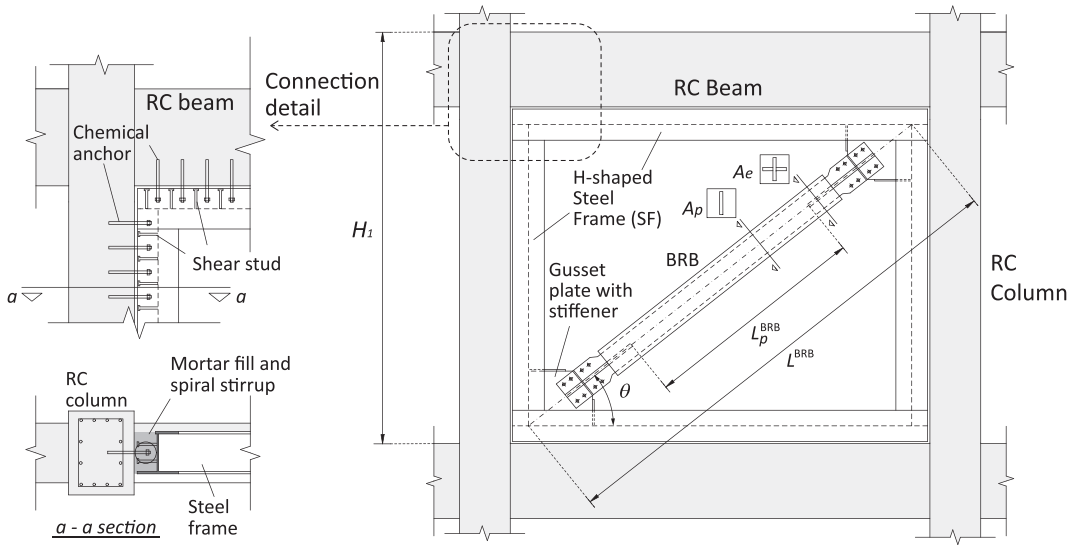

Fig. 1. Simplified layout of BRB application on RC frame, along with connection details.

Richards [8] presented a study comparing the performance of buckling-restrained braced frames and conventional braced frames with eccentric configurations. Prinz and Richards concluded that BRB frames are better than conventional braced frames from a performance standpoint. Takeuchi et al. [9] presented a practical application for retrofitting an existing RC building with both BRBs and an integrated façade, increasing both the seismic and thermal performance of the building simultaneously. However, when the maximum story drift exceeds the yield point of an existing RC frame, all of the structural elements, including BRBs, lose horizontal stiffness. As a result, risk of damage at a specific story and residual deformation after an earthquake is expected. For this situation, a prevention method has not yet been established.

This study evaluates damage distribution and self-centering functions of the elastic steel frame connecting BRBs to RC frames and proposes a simplified method for predicting the seismic performance of a nonlinear RC structure retrofit by BRBs attached via elastic steel frames (SFs) during a major seismic event. Equivalent damping is proposed by idealizing the retrofit building as a linear SDOF system. By extending the SDOF theory, a seismically deficient five-story RC building was digitally modeled and retrofit with BRBs and SFs. Because the BRBs are attached to the existing building through elastically designed steel frames, the effect the elastic member has on reducing the residual displacement was also investigated. Moreover, the same example building was retrofit with CBs for comparison. The proposed method was verified by a multi-degree-of-freedom, nonlinear, time-history analysis using high-intensity earthquake data. The BRB retrofit system responded as predicted and exhibited much smaller drifts than either the un-retrofit original RC frame, or the RC frame retrofit with CBs, ensuring safety during major earthquakes. In addition, the elastic SF reduced the residual displacements to negligible levels.

2. Proposed retrofit design method

The estimated layout of the BRB application model proposed in this study is shown in Fig. 1. BRBs are applied to the RC building by an H-shaped elastic steel frame (SF) working on its weak axis. SF is attached to the RC frame by chemical anchors and shear bolts designed to transfer shear force efficiently. One flange of the SF is half trimmed for the installation of spiral stirrups and mortar fill. The application allows the SF to be included in the computer model as a spring, connected in parallel to the existing RC frame and BRB stiffness. This is a common practice used in Japan [10] and other countries for retrofitting or strengthening existing RC buildings with steel braces or panels, where shear studs are welded to the steel frame and chemical anchors are added via the existing RC frame. Bolts and anchors act as dowels through mortar fill and stirrups, although they are not directly connected. According to the Japanese *Standard for Seismic Diagnosis of Existing Reinforced Concrete Structures* [11], the strength of the connection should be designed to be greater than the lateral load capacity of the SF and the BRB together.

In Fig. 1, H_1 is the story height; θ is the application angle of BRB relative to the horizontal plane; L^{BRB} is the total BRB length; L_p^{BRB} is the plastic core length of BRB; A_p is the cross-sectional area of the plastic core; and A_e is the area of the cruciform cross section, which is assumed to be elastic.

The proposed design method using equivalent linearization was performed using the six steps outlined in the following sections.

2.1. Step 1: Evaluating structural behavior of existing building

The structural behavior of the existing building was evaluated using nonlinear push-over analysis, where obtained push-over curves were substituted with an assumed degrading tri-linear model following the Takeda model [12]. The yield displacement for each story, δ_{yi}^{RC}, was assumed identical for numerical calculation simplicity. Using the mass, M_i^{RC}, and initial stiffness, K_{0i}^{RC}, for each story, eigenvalue analysis is performed and the initial period of the RC building, T_0^{RC}, is obtained.

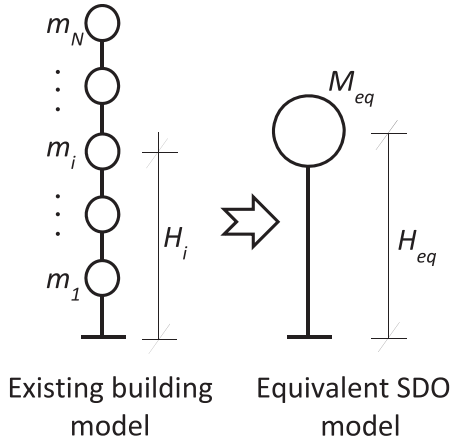

Fig. 2. Equivalent SDOF system.

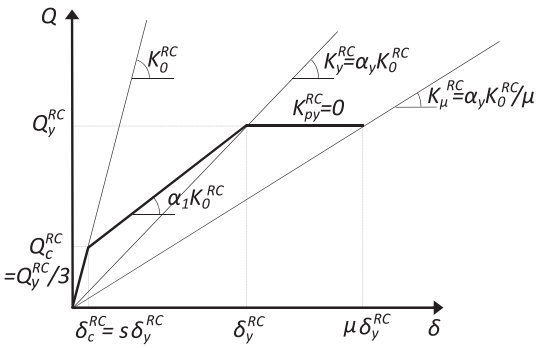

Fig. 3. Degrading tri-linear model for equivalent SDOF RC frame.

2.2. Step 2: Defining an equivalent SDOF model

In this step, an equivalent SDOF model was introduced (Fig. 2).

In Fig. 2, m_i and H_i are the mass and height of the ith floor from ground level, respectively. The equivalent height, H_{eq}, and the equivalent mass, M_{eq}, of the relevant SDOF model are calculated using the following equations:

$$H_{eq}=\frac{\sum_{i=1}^{N} m_i \cdot {}_s u_i \cdot H_i}{\sum_{i=1}^{N} m_i \cdot {}_s u_i} \tag{1a}$$

$$M_{eq}=\frac{\left(\sum_{i=1}^{N} m_i \cdot {}_s u_i\right)^2}{\sum_{i=1}^{N} m_i \cdot {}_s u_i} \tag{1b}$$

where ${}_s u_i$ is the elastic mode component of the ith floor for sth mode. Details of the assumed degrading tri-linear behavior model of the SDOF RC frame are shown in Fig. 3.

In Fig. 3, Q_y^{RC} is the yield shear force, Q_c^{RC} is the crack shear force, δ_y^{RC} is the yield displacement, δ_c^{RC} is the crack displacement, K_0^{RC} is the initial stiffness, K_y^{RC} is the yielding point secant stiffness, K_{py}^{RC} is the post-yielding stiffness, K_μ^{RC} is the post-yielding secant stiffness and μ is the ductility ratio ($\mu=\delta^{RC}/\delta_y^{RC}$). Here, the yield displacement, δ_y^{RC}, is evaluated by scaling δ_{yi}^{RC} proportional to the ratio of the story height, H_{eq}/H_1. As shown in Fig. 3, $Q_c^{RC}=Q_y^{RC}/3$ and $s=\delta_c^{RC}/\delta_y^{RC}=1/10$, and therefore, the post-crack stiffness of the RC frame is equal to $\alpha_1 K_0^{RC}=0.22K_0^{RC}$ and $K_y^{RC}=\alpha_y K_0^{RC}=0.3K_0^{RC}$. Although the push-over results normally exhibit a hardening behavior after yielding, in the proposed BRB design method, the post-yielding phase is assumed as perfectly plastic ($K_{py}^{RC}=0$).

The initial stiffness of the SDOF model, K_0^{RC}, is obtained using the following equation:

$$K_0^{RC}=M_{eq}\left(\frac{2\pi}{T_0^{RC}}\right)^2 \tag{2}$$

The secant stiffness for a random ductility ratio, K_μ^{RC}, can be evaluated using the initial stiffness, K_0^{RC}, with the following equations, where the stiffness reduction coefficient, r, is defined individually for pre-yielding ($s<\mu\le 1$) and post-yielding ($\mu>1$) phases.

$$K_\mu^{RC}=rK_0^{RC} \tag{3.a}$$

$$r=\frac{\alpha_1(\mu-s)+s}{\mu}, \quad s<\mu\le 1 \tag{3.b}$$

$$r=\frac{\alpha_y}{\mu}, \quad \mu>1 \tag{3.c}$$

2.3. Step 3: Evaluating the hysteretic energy dissipated by the RC frame

To evaluate the equivalent damping of the retrofit RC frame, the hysteretic energy dissipated by the RC frame and the BRB is calculated individually. ΔW^{RC} is the hysteretic dissipated energy within the area of the RC frame hysteresis loop for a single cycle and is defined for pre-yielding and post-yielding phases, separately, as shown in Fig. 4(a) and (b).

The unloading stiffness, K_u, for pre-yielding and post-yielding phases is defined according to the Takeda degrading tri-linear model [12], as follows:

$$K_u=\frac{Q_c^{RC}+Q^{RC}}{\delta_c^{RC}+\mu\,\delta_y^{RC}}=K_0^{RC}\,\frac{2s+\alpha_1(\mu-s)}{\mu+s}, \quad s<\mu\le 1 \tag{4.a}$$

$$K_u=\frac{Q_c^{RC}+Q_y^{RC}}{\delta_c^{RC}+\delta_y^{RC}}\cdot\frac{1}{\mu^a}=K_0^{RC}\,\frac{\alpha_y+s}{(1+s)\mu^a}, \quad \mu>1 \tag{4.b}$$

where a is the unloading stiffness degrading parameter (in this study it was assumed that $a=0.4$). Therefore, the hysteretic energy dissipated by the RC frame may be obtained with the following equations:

$$\Delta W^{RC}=2K_0^{RC}\mu^2\left(\delta_y^{RC}\right)^2\frac{r(1-r)s}{s+r\mu}, \quad s<\mu\le 1 \tag{5.a}$$

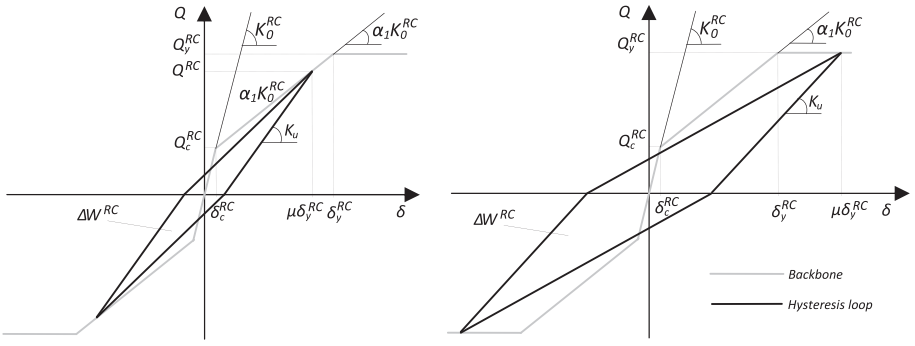

a) Pre-yielding (μ≤1) b) Post-yielding (μ>1)

Fig. 4. Typical hysteresis loops for RC frame.

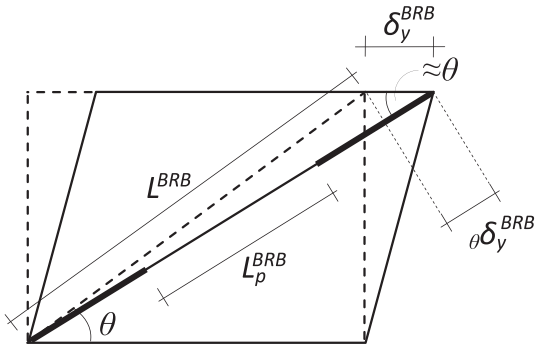

Fig. 5. Evaluation of BRB yielding displacement, δ_y^{BRB}.

$$\Delta W^{RC} = 2rK_0^{RC}\mu^2\left(\delta_y^{RC}\right)^2\left(\frac{r\mu - r(1+s)\mu^a + s}{s+r\mu}\right),\ \mu>1 \tag{5.b}$$

2.4. Step 4: Evaluating the hysteretic energy dissipated by BRBs and effect of elastic SF

The yield point of BRB δ_y^{BRB} is a key parameter for energy dissipation, and for the evaluation of δ_y^{BRB}, new parameters, namely, the plastic core length ratio, $C_P = L_P^{BRB}/L^{BRB}$, and the elastic-to-plastic cross-sectional area ratio, $C_A = A_e/A_P$ are defined.

In Fig. 5, $_\theta\,\delta_y^{BRB}$ is the yield deformation of BRB in the axial direction, and δ_y^{BRB} is the RC frame horizontal displacement that results in BRB yielding. $_\theta\,\delta_y^{BRB}$ can be defined using Eq. (6). In Fig. 5, the parameters shown represent values for a typical story; however, in the following equation, BRB length, L^{BRB}, is converted to SDOF size by scaling-up via H_{eq}/H_1.

$$_\theta\delta_y^{BRB} = \frac{H_{eq}}{H_1}\left(\frac{L_P^{BRB}}{EA_P} + \frac{L^{BRB}-L_P^{BRB}}{EA_e}\right)\sigma_y A_P = \frac{(C_A C_P - C_P + 1)}{C_A}\frac{H_{eq}}{H_1}L^{BRB}\varepsilon_y^{BRB} \tag{6}$$

In Eq. (6), E is the elastic modulus and ε_y^{BRB} is the yield strain for the BRB core material. It should be noted that in practical applications, the value of C_P varies between 0.25 and 0.75, whereas C_A varies between 2.0 and 2.5. Assuming the change in θ caused by frame displacement is neglected, δ_y^{BRB}can be evaluated using Eq. (7):

$$\delta_y^{BRB} \cong_\theta \delta_y^{BRB}/cos\theta \tag{7}$$

The BRB yield displacement, δ_y^{BRB}, is approximately equal to 1/750–1/1000 rad story drift. The force–displacement relation of the BRB is assumed to be elastic–perfectly plastic (Fig. 6). In this step, the amount of BRB is selected using the K^{BRB}/K_0^{RC} ratio, which is the ratio of BRB stiffness to the initial stiffness of the RC frame. In actual practice, K^{BRB}/K_0^{RC} varies between 1.0 and 3.0. With an initially assumed BRB stiffness, the hysteretic energy dissipated by BRB, ΔW^{BRB}, is evaluated using the following equation:

$$\Delta W^{BRB} = 4K^{BRB}\left(\mu^{BRB}-1\right)\left(\delta_y^{BRB}\right)^2,\ \mu^{BRB}>1 \tag{8}$$

where μ^{BRB} is the BRB ductility ratio ($\mu^{BRB} = \mu\,\delta_y^{RC}/\,\delta_y^{BRB}$). The equivalent stiffness of BRB for a random ductility ratio, K_μ^{BRB}, is evaluated using the following equation:

$$K_\mu^{BRB} = K^{BRB}/\mu^{BRB} \tag{9}$$

The total stiffness of the retrofit RC building is evaluated including the effects due to SF. Designed to remain elastic within the target range, SF does not dissipate hysteretic energy but contributes to the total stiffness of the system (Fig. 6). In this study, the stiffness of steel frame, K^{SF}, is indicated relative to BRB stiffness, and in actual practice, the ratio of the steel frame to BRB stiffness ($\gamma_s = K^{SF}/K^{BRB}$) varies between 0.04 and 0.10.

The Japanese *Manual for Design and Construction of Passively-Controlled Buildings* [13] recommends that the shear strength of additional dampers in a structure should correspond to a base shear

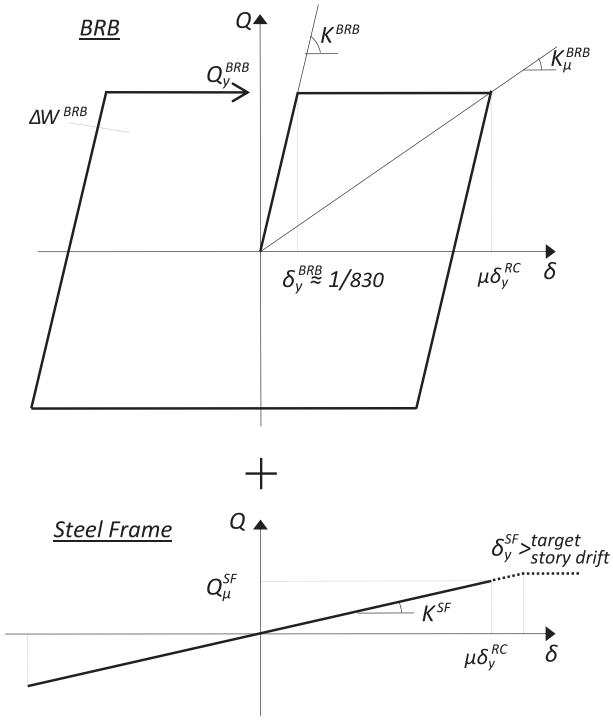

Fig. 6. BRB and SF force–displacement relations.

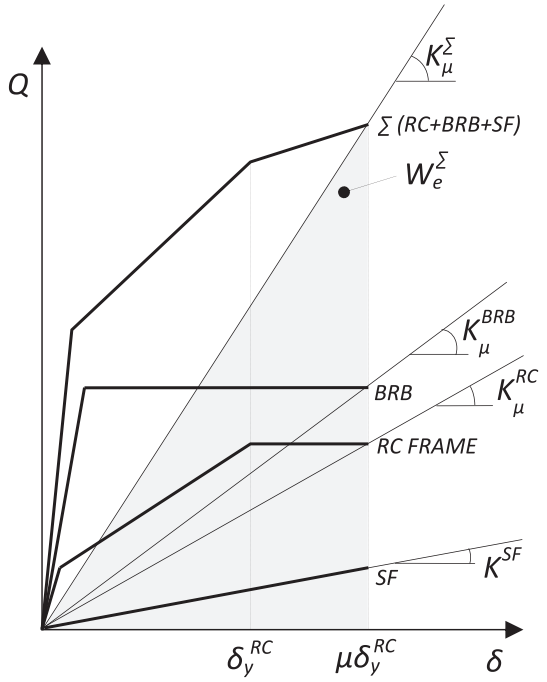

Fig. 7. Overall behavior of SDOF model with BRB.

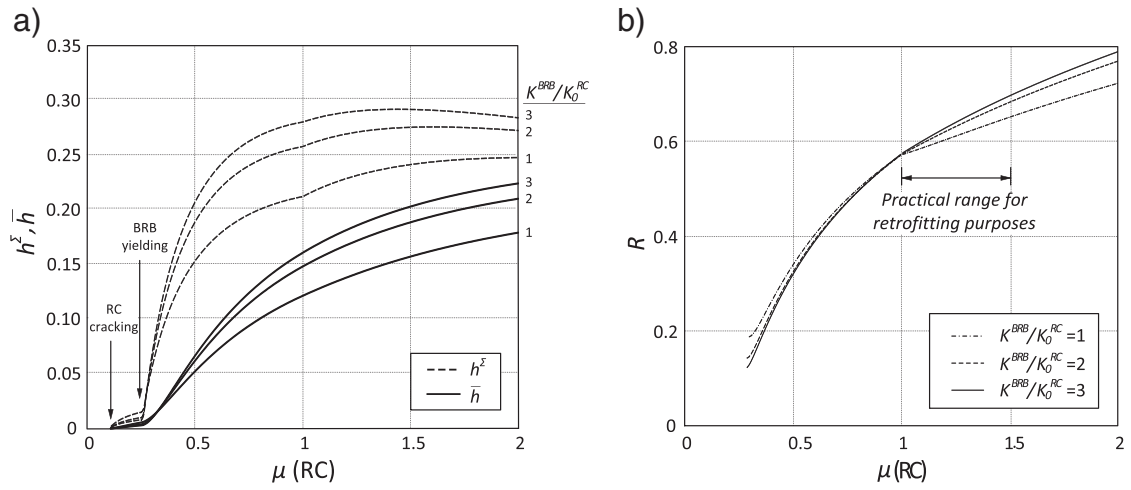

Fig. 8. (a) Comparison of total damping and average damping (b) Damping reduction factor, *R*.

coefficient of approximately 30%. Following this recommendation, an initial value of K^{BRB}/K_0^{RC} ratio can be assumed with the following equation:

$$K^{BRB}/K_0^{RC} = \frac{C_b W_{eq}}{K_0^{RC}\left(\delta_y^{BRB} + \gamma_s \mu_t \delta_y^{RC}\right)} \tag{10}$$

where C_b is the base shear coefficient recommended by the relevant code, W_{eq} is the equivalent weight of the building and $\mu_t$is the target ductility of the retrofitting project.

2.5. Step 5: Evaluating equivalent damping ratio of retrofit system, h_{eq}

The skeleton curve of the retrofit structural behavior is shown in Fig. 7. In this figure, K_μ^Σ is the equivalent stiffness of the total system (RC + BRB + SF) corresponding to a random ductility value and can be evaluated by the following two equations:

$$K_\mu^\Sigma = K_\mu^{RC} + K^{BRB} + K^{SF},\ \mu^{BRB} \le 1 \tag{11.a}$$

$$K_\mu^\Sigma = K_\mu^{RC} + K_\mu^{BRB} + K^{SF},\ \mu^{BRB} > 1 \tag{11.b}$$

In Fig. 7, W_e^Σ is the equivalent potential energy of the RC frame with BRB and SF. It is evaluated as follows:

$$W_e^\Sigma = \frac{1}{2} K_\mu^\Sigma \left(\mu \delta_y^{RC}\right)^2 \tag{12}$$

The total equivalent hysteretic damping ratio of the SDOF RC model and equivalent BRB model, $h^\Sigma = h^{RC} + h^{BRB}$, is expressed by Eq. (13), which is based on the equivalent damping expression of the resonant steady state [14].

$$h^\Sigma = \frac{\Delta W^{RC} + \Delta W^{BRB}}{4\pi W_e^\Sigma} \tag{13}$$

Because a structure exhibits a large number of hysteresis loops with diverse amplitudes during an earthquake excitation, Newmark and Rosenbluth [15] proposed an average damping concept, which evaluates the average damping for a range from zero to maximum amplitude. The average damping is calculated using Eq. (14).

$$\bar{h} = \frac{1}{\mu_t}\int_0^{\mu_t} h^\Sigma d\mu \tag{14}$$

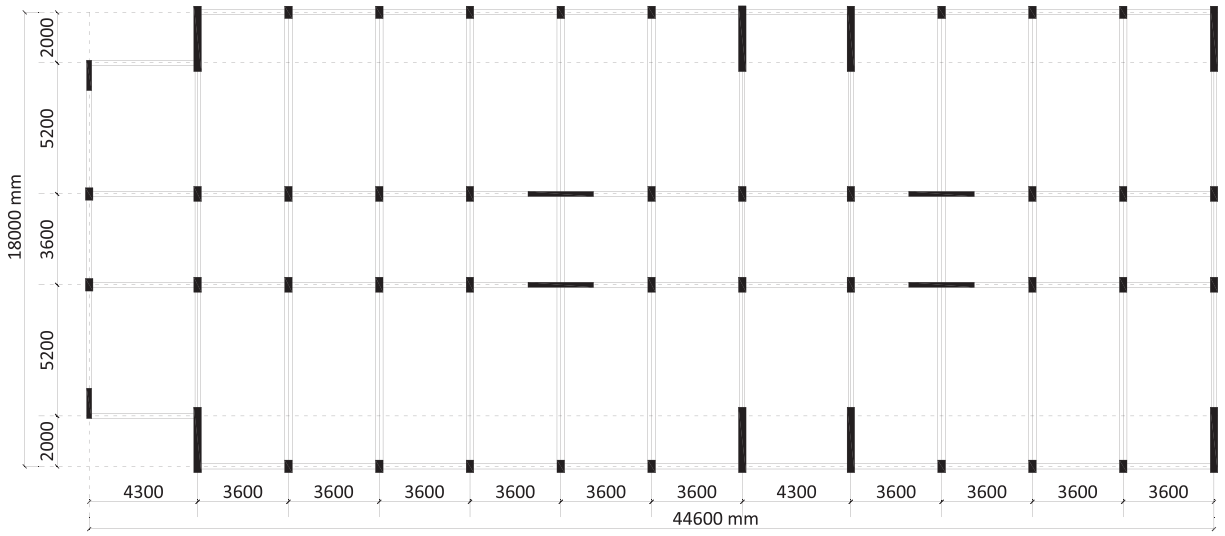

Fig. 9. Plan of RC school building in Turkey.

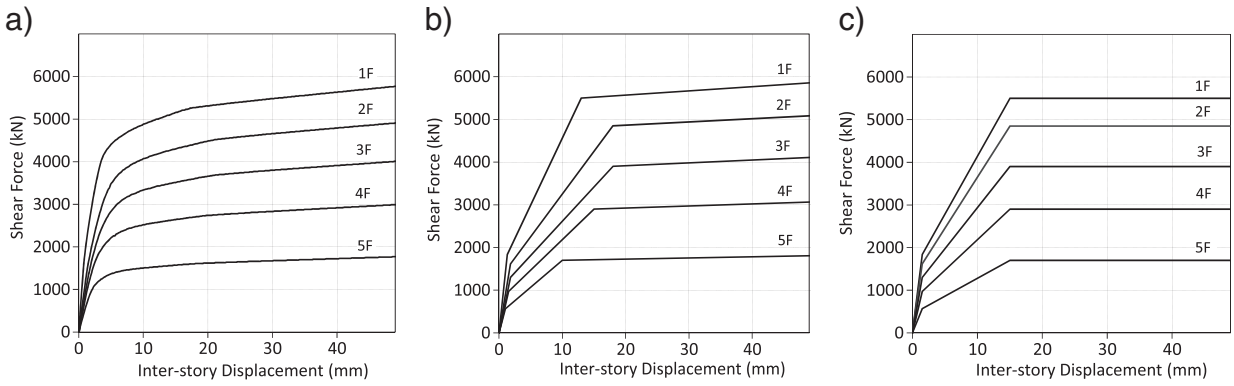

Fig. 10. (a) Push-over curves for model building. (b) Substitute degrading tri-linear behavior. (c) Simplified tri-linear behavior.

In Fig. 8(a), the total damping, h^{Σ}, is compared with the average damping, $\overline{h}$. A damping reduction factor, R, representing the decreased damping via the average damping method, is proposed, as shown in Eq. (15) and in Fig. 8(b).

$$\overline{h} = Rh^{\Sigma} \tag{15}$$

In this study, considering the practical range of target ductility for retrofitting RC buildings, the damping reduction factor, R, was assumed to be 60%. Finally, the equivalent damping ratio for the overall system, h_{eq}, is evaluated with Eq. (16). In this equation, h_f represents the inherent structural damping ratio that is proportional to the instantaneous tangential stiffness and is assumed as $h_f = 0.03$.

$$h_{eq} = h_f + \overline{h} \tag{16}$$

2.6. Step 6: Evaluating the amount of BRB for retrofitting

Because the equivalent stiffness of the retrofit system, K_{μ}^{Σ}, has already been evaluated, the equivalent period of the retrofit system, T_{μ}^{Σ}, is obtained with the following equation:

$$T_{\mu}^{\Sigma} = T_0^{RC}\sqrt{\frac{K_0^{RC}}{K_{\mu}^{\Sigma}}} \tag{17}$$

In this step, using the equivalent damping ratio, h_{eq}, and the equivalent period of the retrofit system, T_{μ}^{Σ}, the spectral displacement, $S_D(T_{\mu}^{\Sigma}, h_{\mu}^{\Sigma})$, is calculated for the relevant design spectrum or a selected ground motion. If the evaluated displacement response does not satisfy the target drift ratio for the SDOF model, the amount of BRB is re-adjusted in Step 4 until a satisfactory result is obtained. Finally, the stiffness of designed BRB for each story, K_i^{BRB}, is calculated according to the ratio K^{BRB}/K_0^{RC}, as shown in the following equation:

$$K_i^{BRB} = \left(K^{BRB}/K_0^{RC}\right)K_{0i}^{RC} \tag{18}$$

3. Original five-story RC building and response reduction

A typical five-story RC school building in Turkey, with a common floor plan, was used for validation of the proposed method (Fig. 9). This particular school building was constructed in 1992 in Istanbul, which is a high-risk seismic zone. The story height for each level is identical, $H_1 = 3.2$ m. The average concrete compressive strength is 20 MPa, and the reinforcement bar steel strength is 220 MPa. Today, neither structural member section sizes nor the amount of reinforcement bars satisfies the current design code. In this study, an investigation of the building and assessment of its structural performance, both before and after BRB retrofit, was performed in the longitudinal direction only, because this is the weaker direction.

Limits regarding target story drift are given in several documents. In the NEHRP *Commentary on the Guidelines for Rehabilitation of Buildings* (FEMA 273) [16], successive FEMA 356 guidelines [17], and ATC-40 [16], the maximum story drift angle regarding immediate occupancy performance level is stated as 1/100. However, the Japanese *Standard for Seismic Diagnosis of Existing Reinforced Concrete Structures* [18] recommends 1/150. In the present study, the target story drift angle was assumed to be 1/150 rad.

The push-over analysis results for the sample school building are given in Fig. 10(a). These curves are converted into a tri-linear degrading model, as shown in Fig. 10(b). The converted tri-linear models for each story are assumed such that the elastically absorbed energy is equivalent of the original push-over curves. Finally, assumed tri-linear models used in this study are further simplified, which assumes identical yielding displacements for each floor and a perfectly plastic post-yielding phase, as shown in Fig. 10(c) and as summarized in Table 1. Using eigenvalue analysis, the initial period of the structure was calculated as $T_0 = 0.7$ s, whereas the equivalent height and equivalent mass of the structure were calculated using Eqs. (1a) and (1b), with $H_{eq} = 10.5$ m and $M_{eq} = 4433.5$ tons, respectively. Because the target story drift angle was assumed as 1/150 rad, the target ductility was $\mu_t = 1.42$, and using Eq. (2), the initial stiffness of the SDOF RC model was calculated as $K_0^{RC} = 356.8$ kN/mm.

BRBs with a core cross-sectional area of $A_p = 55.5$ cm^2 and material yield strength of $\sigma_y = 225$ N/mm^2 were selected. The steel frame used to attach the BRB to the RC frame is of W10 × 10 × 49 (H-250 × 250 × 9 × 14) section, and its material yield strength is $\sigma_{y-sf} = 325$ N/mm^2. The plastic core length ratio and the elastic–to–plastic cross-sectional ratio were assumed to be $C_P = 0.5$ and $C_A = 2.5$, respectively. The BRB application angle is $\theta = 36.4°$, which gives an SF-to-BRB stiffness ratio of $\gamma_s = 0.047$. Using Eq. (10), the initial value of K^{BRB}/K_0^{RC} was selected as 2.25, which corresponds to the total shear strength of BRB and SF relative to 30% of the base-shear force. Equivalent damping of the retrofit system was found to be $h_{eq} = 0.22$, and the equivalent period was $T_{\mu}^{\Sigma} = 0.81$ s. Regarding the design seismic wave, BCJ-L2 from the Japanese design code was used, which is an artificial wave generated

Table 1
Simplified tri-linear behavior values and story weight for model building.

Floor	K_{0i}^{RC} (kN/mm)	δ_{ci}^{RC} (mm)	Q_{ci}^{RC} (kN)	δ_{yi}^{RC} (mm)	Q_{yi}^{RC} (kN)	W_i (kN)
5 F	377.8	1.5	556.7	15	1700.0	5397.0
4 F	644.4	1.5	966.7	15	2900.0	11824.0
3 F	866.7	1.5	1300.0	15	3900.0	11824.0
2 F	1077.8	1.5	1616.7	15	4850.0	11824.0
1 F	1222.2	1.5	1833.3	15	5500.0	11824.0

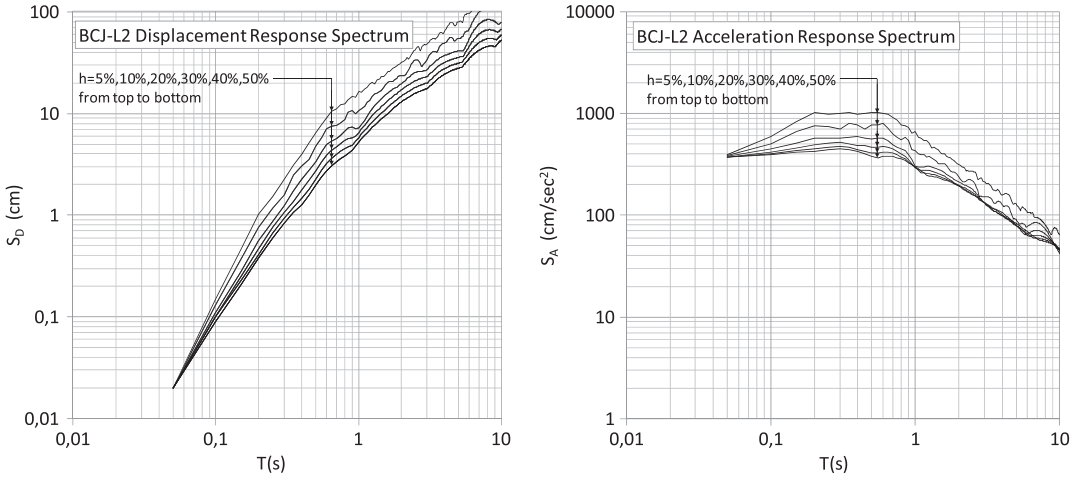

Fig. 11. BCJ-L2 acceleration and displacement response spectrum (h = 5%, 10%, 20%, 30%, 40% and 50%).

to overlap the design spectrum. It corresponds to a 475-year return period earthquake (10% probability in 50 years). The acceleration and displacement response spectrum for BCJ-L2 are given in Fig. 11.

Based on the displacement spectrum of BCJ-L2 ground motion, the relevant displacement response for the equivalent SDOF model was calculated as 6.69 cm, which corresponds to 1/157 story drift. Because the result is satisfactory, the number of BRBs to be used on each floor, n_i^{BRB}, is calculated using Eq. (7), which supports the target shear force using BRBs.

$$n_i^{BRB} = \frac{K_i^{BRB} \cdot \delta_{yi}^{BRB}}{Q_{y1}^{BRB}} \tag{19}$$

where Q_{y1}^{BRB} is the shear force that can be supported by a single BRB, and δ_{yi}^{BRB} is the yield displacement of the BRB, which is evaluated by scaling the value from the SDOF model as $\delta_{yi}^{BRB} = (H_1/H_{eq})\delta_y^{BRB}$.

As an alternative retrofitting method, the identical RC structure was retrofit with conventional braces (CBs), and the nonlinear time-history analysis results were compared. Regarding the CBs, a W8 × 8 × 35 (H-200 × 200 × 8 × 12) section was selected with the same material properties as those of the BRBs. To ensure a consistent comparison, the number of BRBs and CBs on each story, as well as the application angles and the SF properties, was identical (Table 2). For the analysis, CBs were modeled using the Shibata–Wakabayashi buckling model [19]. For the details of the Shibata–Wakabayashi model, please refer to the Appendix A.

The proposed method was verified by nonlinear time-history analysis during the BCJ-L2 seismic wave using a lumped-mass model of the model building for the cases with and without retrofitting. The story stiffness and story weight of the model building is given in Table 1. The stiffness of BRB and SF is included in the computer model as a spring, connected in parallel to the existing RC frame stiffness. The maximum inter-story displacement of the original RC frame (RC only), the RC frame retrofit with the evaluated number of BRB and SF (RC + BRB + SF) members and the RC frame retrofit with CBs (RC + CB + SF) are shown in Fig. 12. The figure also includes the maximum inter-story displacement of the RC frame retrofit with BRB, but without using the SF (RC + BRB) to show the effects of SF bracing. As shown in the figure, after the BRB retrofit, the excessive displacements of the original RC frame were prevented, and the target displacement was no longer exceeded. Owing to the unbalanced hysteresis behavior of the CBs, when the structural response exceeded the buckling strength, the CB retrofit resulted in excessive displacement at the first-story level, as anticipated. Retrofitting with BRBs without using SF also prevented excessive displacements, but the second-story level exceeded the target displacement.

In addition, time-history analyses based on the application of six additional scaled ground motions were performed. The ground motions applied are summarized in Table 3. The ground motions were scaled to match the BCJ-L2 response acceleration spectrum at the target period of the retrofit model, $T_{\mu}^{\Sigma} = 0.81$ s. Fig. 13 shows the unscaled response acceleration spectra of the six ground motion records, in addition to the relevant design earthquake spectrum.

Fig. 14 shows the results of the time-history analysis for individual ground motion records. As seen in the figure, the building model retrofit with the proposed BRB design method does not exceed the target inter-story drift values, except in a limited number of cases, and the mean value of inter-story displacement is smaller than the target drift.

Residual deformation affecting structures during an earthquake provides a common reference for post-earthquake damage assessment [20]. Moreover, McCormick et al. [21] addressed the issue of discomfort of a building's occupants due to residual deformations. McCormick et al. reported significant discomfort felt by occupants of structures with residual inclinations above 1/125 rad story drift and proposed a permissible residual deformation limit of 1/200 rad to be considered in performance-based seismic designs.

Table 2
Number of BRBs and CBs applied per floor.

	BRB cross section	K_L^{BRB} (kN/mm)	n_L^{BRB}	CB cross section	Number of CBs n_L^{CB}
5 F	Plastic core	850	4	W8 x 8 x 35	4
4 F	222mmx26mm	1450	6	A = 6540 mm²	6
3 F	A_p=5550mm²	1950	8		8
2 F		2425	9		9
1 F		2750	11		11

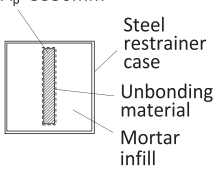

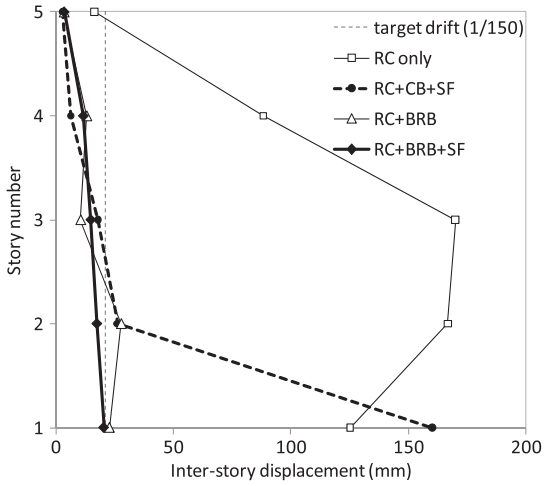

Fig. 12. Maximum inter-story displacement distribution.

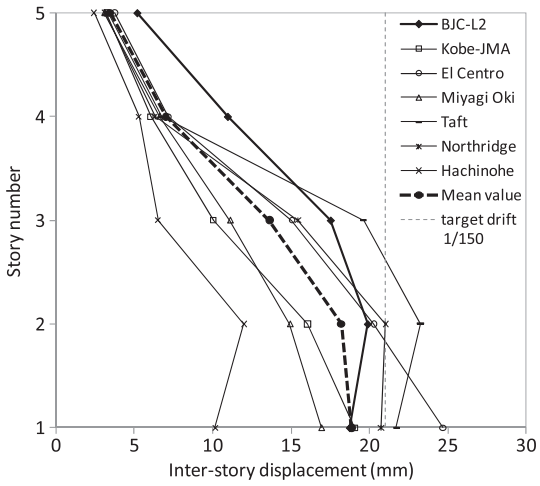

Fig. 14. Maximum inter-story displacement distribution for selected earthquakes and mean inter-story displacement.

Table 3
Ground motion records used for dynamic time-history analysis.

Input motion	PGA (cm/s^2)	S_A at T_{μ}^{Σ}=0.81 s (cm/s^2)	Input intensity (%)
Kobe-JMA (N-S)	817.85	1868.91	40.1
El Centro (N-S)	341.78	537.55	139.6
Miyagi Oki 1978 (N-S)	206.40	555.33	135.1
Taft-Kent County (E-W)	174.42	297.92	251.9
Northridge-Sylmar (N-S)	826.80	431.82	173.8
Hachinohe-Tokachi (E-W)	176.58	618.21	121.4
BCJ-L2	355.66	750.33	100.0

In the method proposed, if SF elements remain elastic within the target story drift range, they improve the self-centering capacity of the building and reduce residual displacement, especially after a severe earthquake motion of long duration. In Fig. 15, the inter-story displacement time-history of the second story is shown for the "RC only" model, RC + BRB + SF model and a model representing a BRB-retrofit RC frame, but without the SF component (RC + BRB). Compared to the "RC only" model, the RC + BRB model exhibits no significant residual displacements following an earthquake. Nonetheless, addition of the SF component essentially eliminates residual displacements.

IDA analysis [22] was run to assess the structural performance under increasing values of earthquake input intensity; the results are shown in Fig. 16(a) and (b). As shown in Fig. 16(a), retrofitting with BRBs and CBs gives similar results up to 0.2 g input intensity, at which point CBs start buckling. Additionally, for increasing ground motion intensities, the building retrofit with CBs exhibits insufficient performance. The model retrofit with BRBs exhibits a stable behavior even for intensities greater than 1 g, which is the design intensity of the BRB used in this study. Fig. 16(b) shows the IDA curves for maximum residual displacement, indicating that residual displacement of the RC building retrofit with CBs exceeds acceptable values for input intensities greater than 0.6 g. Even at 1 g input levels, the RC + BRB + SF model attains less than 1/2000 rad residual drift, which is of negligible influence.

4. Conclusions

Based on this study's findings, although retrofitting of existing RC frames using BRBs improves seismic performance relative to conventional retrofitting techniques, a simplified design method and stability after RC frame yielding is an issue that must still be solved. This paper defines an elastic steel frame connecting BRBs to RC frames as a key element that prevents damage concentration at a specific story and reduces residual deformation In addition, a simplified equivalent linearization method to evaluate the amount of BRB and SF was proposed. The results were confirmed by nonlinear time-history analysis and the

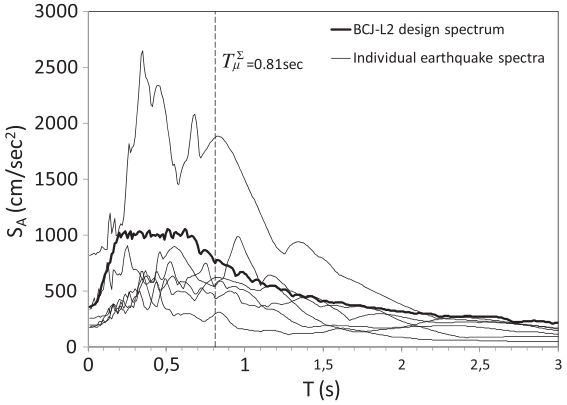

Fig. 13. BCJ-L2 design spectra and individual earthquake spectra.

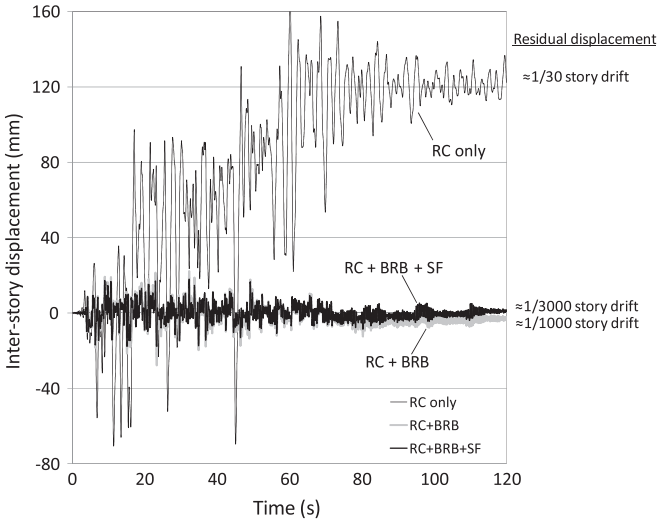

Fig. 15. Inter-story displacement time-history (2nd story).

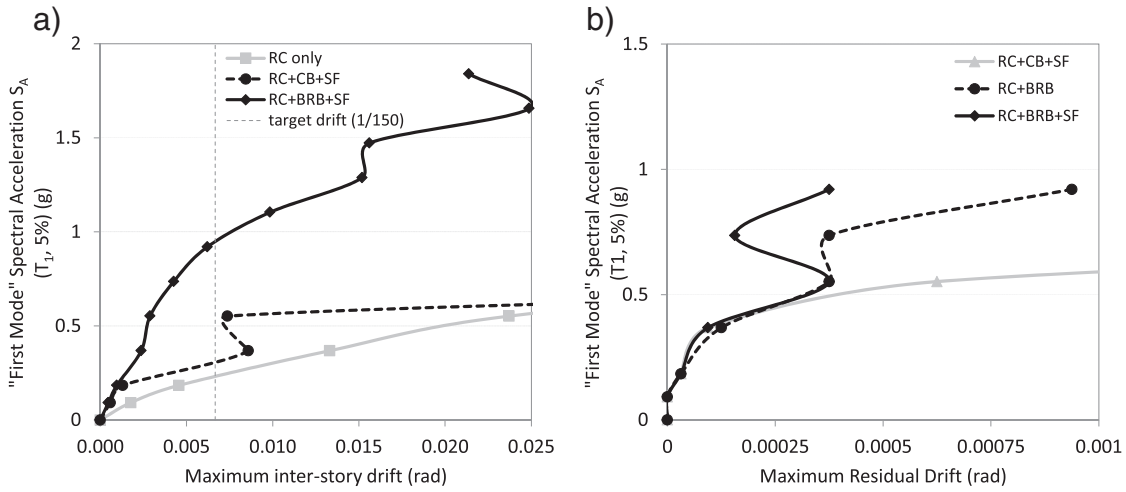

Fig. 16. IDA curves for (a) maximum inter-story drift angle and (b) maximum residual drift angle.

accuracy of the proposed method was validated. The conclusions of this study are as follows:

1. The results of the proposed BRB retrofit design method were compared with the retrofit method using conventional braces. Because conventional braces exhibit unbalanced hysteresis behavior and buckle before tensile yielding occurs, damage concentration at a specific story can result. This suggests and confirms the principal and undeniable advantage of BRBs over conventional braces.
2. Time-history analysis results indicate that an RC building retrofit with BRB + SF responds according to predictions of the proposed design method and with greatly decreased story drift.
3. Residual displacement of the RC frame is significantly reduced with the application of BRBs using elastic steel frames. The results showed that as the elastic range of SF is designed beyond the target story drift, the self-centering function of SF is able to reduce residual displacements to negligible levels.
4. IDA analysis proved that existing RC buildings retrofit with BRB and SF exhibit reliable performance for increasing values of ground motion intensity. The original RC frame loses seismic capacity gradually in the same analysis, whereas RC frames retrofit with CBs exhibit a sudden drop in seismic performance as soon as buckling occurs in the braces.
5. The proposed method and nonlinear time-history verification analysis assumed a lumped-mass model for simplicity. In actual practice, in addition to evaluating the required amount of BRB and SF for any retrofit, the location of the BRBs in the building plan is of key importance. Placing the BRBs on axis with the perimeter of the building will not only prevent torsional effects during a potential ground motion but also offer easy implementation options, enabling most areas of the building to remain occupied and operational during ongoing retrofit implementation.

The proposed method is particularly recommended for schools, hospitals, and other public buildings considering their importance and safety needed during and after an earthquake and also the ease of proposed retrofitting application owing to the relatively symmetrical plan of such buildings.

The issues of local weaknesses of certain stories (weak story) or buildings with plan irregularities are further subjects to be discussed.

Appendix A. Shibata–Wakabayashi model for conventional brace hysteresis behavior

A summary of the Shibata–Wakabayashi model for conventional braces (Wakabayashi et al., 1977) is shown in Fig. A1 below. The normalized hysteresis behavior of a CB is represented and the critical points are given below.

In Fig. A1, δ is the normalized strain, n is the normalized axial force, N_y is the axial yielding force, Δ_y is the axial yield strain, A is the tension yielding critical point, B is the compression buckling critical point, P is the partial tensile yielding critical point and Q is the release point following the buckling path. The normalized axial force, n, for the relevant phase is given by Eq. (A.1), and the related parameters in Eq. (A.1) are obtained using Eqs. (A.2)–(A.6).

$$n = \begin{cases} 1 & [\text{Phase A}] \\ f_t\left(\delta^A - \delta\right) & [\text{Phase B}] \\ n^P + \dfrac{\left(\delta - \delta^P\right)\left(n^P - n^Q\right)}{\left(\delta^P - \delta^Q\right)} & [\text{Phase C}] \\ -f_c\left(\delta^B + n^C - \delta\right) & [\text{Phase D}] \end{cases} \tag{A.1}$$

$$f_c(X) = (p_1 X + p_2)^{-0.5} \tag{A.2}$$

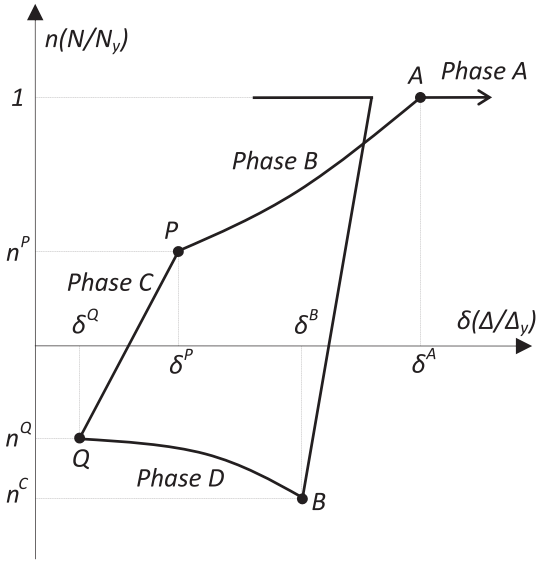

Fig. A1. Shibata–Wakabayashi model for the definition of conventional buckling brace hysteresis behavior.

$$f_t(X) = (p_3 X + 1)^{-1.5} \tag{A.3}$$

$$p_1 = \left(\frac{10\lambda^2\sigma_y}{3\pi^2 E} - 0.\overline{3}\right) \tag{A.4}$$

$$p_2 = \left(\frac{4\lambda^2\sigma_y}{\pi^2 E} + 0.6\right) \tag{A.5}$$

$$p_3 = \frac{1}{\left(\frac{3.1\pi^2 E}{\lambda^2\sigma_y} + 1.4\right)} \tag{A.6}$$

where σ_y is the material yield stress, λ is the slenderness ratio of the brace, and E is the elastic modulus. If the phase changes, the reference points A, B, P and Q are defined with the following equations:

[Release in Phase B]

$$\begin{cases} \delta^B_{\text{new}} = \delta^B_{\text{old}} + \left(\delta^A - 1 - n^C - \delta^B_{\text{old}}\right)\dfrac{\delta - \delta^p_{\text{old}}}{\delta^A - \delta^p_{\text{old}}} \\ \delta^p_{\text{new}} = \delta \\ n^p_{\text{new}} = n \\ \delta^Q_{\text{new}} = \delta^B_{\text{new}} - \dfrac{\left(\delta^A - \delta\right)}{q_3} \\ n^Q_{\text{new}} = -f_c\left(\delta^B_{\text{new}} + n^C - \delta^Q_{\text{new}}\right) \end{cases} \tag{A.7}$$

$$\begin{cases} q_3 = 0.3\sqrt{n_E} + 2.4 \\ n_{\text{E}} = \dfrac{\pi^2 E}{\lambda^2\sigma_y}\left(\text{Euler Buckling Stress},\ \lambda : \text{Slenderness Ratio}\right) \end{cases} \tag{A.8}$$

[Release in Phase C]

$$\begin{cases} \delta^A_{\text{new}} = \delta^A_{\text{old}} + \ln\left\{q_1\left(\delta^D - \delta\right) + 1\right\} - q_2\left(\delta^B - \delta^D\right) \geq \delta^A_{\text{old}} \\ \delta^Q_{\text{new}} = \delta \\ n^Q_{\text{new}} = n \\ \delta^P_{\text{new}} = \delta^A_{\text{new}} - q_3\left(\delta^B - \delta\right) \\ n^P_{\text{new}} = f_t\left(\delta^A_{\text{new}} - \delta^P_{\text{new}}\right) \end{cases} \tag{A.9}$$

$$\begin{cases} q_1 = \left(3 - \dfrac{1}{n_E}\right)/10 \\ q_2 = \dfrac{0.115}{n_E} + 0.36 \end{cases} \tag{A.10}$$

[Release in Phase A]

$$\begin{cases} \delta^A_{new} = \delta^P_{new} = \delta \\ n^P_{new} = 1 \\ \delta^B_{new} = \delta^Q_{new} = \delta - 1 - n_c \\ n^Q_{new} = -n_c \end{cases} \tag{A.11}$$

References

[1] Kasai K, Fu Y, Watanabe A. Passive control systems for seismic damage mitigation. J Struct Eng 1998;124(5):501–12.
[2] Takeuchi T, Kasai K, Oohara K, Kimura Y, Nakashima H. Performance evaluation and design of passively controlled building using equivalent linearization. SEWC 2002 Conference Proceedings, Yokohama, Japan; 2002.
[3] Ichikawa Y, Takeuchi T, Morimoto S, Sugiyama M. Practical design of high-rise structure using viscoelastic dampers and hysteretic dampers. SEWC 2002 Conference Proceedings, Yokohama, Japan; 2002.
[4] Kuramoto H, Iiba M, Wada A. A seismic evaluation method for existing reinforced concrete buildings retrofitted by response controlling techniques. J Struct Constr Eng Trans AIJ 2002;559:189–95 [In Japanese].
[5] Choi H, Kim J. Energy-based design of buckling-restrained braced frames using hysteretic energy spectrum. Eng Struct 2006;28:304–11.
[6] Sahoo DR, Chao S-H. Performance-based plastic design method for buckling-restrained braced frames. Eng Struct 2010;32:2950–8.
[7] Pu W, Kasai K. Passive control design method for RC building structure added with elasto-plastic damper. J Struct Constr Eng Trans AIJ 2013;78(685):461–70 [In Japanese].
[8] Prinz GS, Richards PW. Seismic performance of buckling-restrained braced frames with eccentric configurations. J Struct Eng ASCE 2012;138(3):345–53.
[9] Takeuchi T, Yasuda K, Iwata M. Studies on integrated building facade engineering with high-performance structural elements. IABSE Symposium Budapest 2006; 2006.
[10] Fukuyama H, Sugano S. Japanese seismic rehabilitation of concrete buildings after the Hyogoken-Nanbu earthquake. Cement Concr Compos 2000;22:59–79.
[11] Standard for Seismic Diagnosis of Existing Reinforced Concrete Structures—English Version. The Japan Building Disaster Prevention Association; 2001.
[12] Takeda T, Sozen MA, Nielsen NN. Reinforced concrete response to simulated earthquakes. J Struct Div ASCE 1970;96(12):2557–73.
[13] Manual for Design and Construction of Passively-Controlled Buildings. 2nd ed. Japan Society of Seismic Isolation; 2005 [In Japanese].
[14] Jacobsen LS. Damping in Composite Structures. 2nd World Conference on Earthquake Engineering, Japan; 1960. p. 1029–44.
[15] Newmark NM, Rosenblueth E. Fundamentals of Earthquake Engineering. New Jersey: Prentice-Hall Inc.; 1971.
[16] FEMA 273. NEHRP Guidelines for the Seismic Rehabilitation of Buildings, FEMA 273. Prepared for FEMA by the Applied Technology Council and the Building Seismic Safety Council. Washington, DC: Federal Emergency Management Agency; 1997.
[17] FEMA 356. Prestandard and Commentary for the Seismic Rehabilitation of Buildings, FEMA 356. Prepared for FEMA by the American Society of Civil Engineers. Washington, DC: Federal Emergency Management Agency; 2000.
[18] ATC 40 Report, Seismic Evaluation and Retrofit of Concrete Buildings. Applied Technology Council; 1996.
[19] Shibata M, Wakabayashi M. Mathematical expression of hysteretic behavior of braces—part 2 application of dynamic response analysis. Trans AIJ 1982;320:29–35 [In Japanese].
[20] Yazgan U, Dazio A. Post-earthquake damage assessment using residual displacements. Earthq Eng Struct Dyn 2012;41:1257–76 [2012].
[21] McCormick J, Aburano H, Ikenaga M, Nakashima M. Permissible Residual Deformation Levels for Building Structures Considering Both Safety and Human Elements. 14th World Conference on Earthquake Engineering, Beijing, China; 2008.
[22] Vamvatsikos D, Cornell CA. Incremental dynamic analysis. Earthq Eng Struct Dyn 2002;31(3):491–514.